

UC Davis

UC Davis Previously Published Works

Title

Antimelanoma Effects of Concomitant Inhibition of SIRT1 and SIRT3 in BrafV600E/PtenNULL Mice.

Permalink

<https://escholarship.org/uc/item/92z073pb>

Journal

Journal of Investigative Dermatology, 142(4)

Authors

Chhabra, Gagan

Singh, Chandra

Guzmán-Pérez, Glorimar

et al.

Publication Date

2022-04-01

DOI

10.1016/j.jid.2021.08.434

Peer reviewed



Published in final edited form as:

*J Invest Dermatol.* 2022 April ; 142(4): 1145–1157.e7. doi:10.1016/j.jid.2021.08.434.

## Anti-melanoma effects of concomitant inhibition of SIRT1 and SIRT3 in *Braf*<sup>V600E</sup>/*Pten*<sup>NULL</sup> mice

Gagan Chhabra<sup>1,#</sup>,  
Chandra K. Singh<sup>1,#</sup>,  
Glorimar Guzmán-Pérez<sup>1,#</sup>,  
Mary A. Ndiaye<sup>1</sup>,  
Kenneth A. Iczkowski<sup>2</sup>,  
Nihal Ahmad<sup>1,3,\*</sup>

<sup>1</sup>Department of Dermatology, University of Wisconsin, Madison, Wisconsin, USA

<sup>2</sup>Department of Pathology, Medical College of Wisconsin, Milwaukee, Wisconsin, USA

<sup>3</sup>William S. Middleton VA Medical Center, Madison, Wisconsin, USA

### Abstract

Novel therapeutic strategies are required for the effective and lasting treatment of metastatic melanoma, one of the deadliest skin malignancies. In this study, we determined the anti-melanoma efficacy of 4'-bromo-resveratrol (4'-BR), which is a small molecule dual inhibitor of SIRT1 and SIRT3 in a *Braf*<sup>V600E</sup>/*Pten*<sup>NULL</sup> mouse model that recapitulates human disease, including metastases. Tumors were induced by topical application of 4-hydroxy-tamoxifen on shaved backs of 10-week-old mice, and the effects of 4'-BR (5-30 mg/kg b.wt.; intraperitoneally; 3d/week for 5 weeks) were assessed on melanoma development and progression. We found that 4'-BR at a dose of 30 mg/kg significantly reduced size and volume of primary melanoma tumors, as well as lung metastasis, with no adverse effects. Further, mechanistic studies on tumors showed significant modulation in markers of proliferation, survival and melanoma progression. As SIRT1 and SIRT3 are linked to immunomodulation, we performed differential gene expression analysis via NanoString PanCancer Immune Profiling panel (770 genes). Our data demonstrated that 4'-BR significantly downregulated genes related to metastasis-promotion, chemokine/cytokine-regulation, and innate/adaptive immune functions. Overall, inhibition of SIRT1 and SIRT3 by 4'-BR is a promising anti-melanoma therapy with anti-metastatic and immunomodulatory activities warranting further detailed studies, including clinical investigations.

\*Correspondence to: Nihal Ahmad, Ph.D., Department of Dermatology, University of Wisconsin-Madison, Wisconsin Institutes for Medical Research, 1111 Highland Avenue, Room 7045, Madison, WI 53705; Phone: (608) 263-5359; Fax: (608) 262-7137; nahmad@dermatology.wisc.edu.

#Equal contributions

#### CRedit STATEMENT

Conceptualization: GC, CS, MN, NA; Data curation: GC, CS, GG; Formal Analysis: GC, CS, MN, GG, KI; Funding Acquisition and Resources: NA; Investigation: GC, CS, GG, NA; Methodology: GC, CS, MN, GG; Supervision: NA; Validation: GC, CS, GG; Visualization: GC, CS, GG; Writing - Original Draft Preparation: GC, CS, GG; Writing - Review and Editing: GC, CS, GG, MN, KI, NA.

#### CONFLICT OF INTEREST

The authors state no conflict of interest.

## Keywords

Melanoma; SIRT1; SIRT3; Bromo-resveratrol; Nanostring

---

## INTRODUCTION

Recent advances in the understanding of melanoma biology have led to the development of promising targeted therapies. The BRAF inhibitors vemurafenib and dabrafenib achieved significant improvement over traditional chemotherapy and were approved for patients with metastatic melanomas harboring BRAF-mutations. More recently, the combination of dabrafenib with the MEK inhibitor trametinib demonstrated improved progression-free survival as compared to monotherapy, and has received approval from the US FDA. However, even with the combination treatment, most patients develop resistance, thereby failing to achieve lasting tumor regression (Flaherty et al., 2012, Gowrishankar et al., 2012). Interestingly, melanoma has been characterized as one of the most immunogenic tumors and immune-targeted therapeutics have been successful and approved for melanoma treatment. However, the high rates of resistance acquisition, large percentage of partial responders and lack of durable responses remain obstacles to the success of these therapies (Jenkins and Fisher, 2020). Since melanoma is notoriously resistant to treatment and current therapeutic approaches have not been able to effectively manage this neoplasm, additional novel target-based approaches are needed.

The mammalian sirtuins (SIRT) constitute a family of seven known members (SIRT1 – SIRT7) with NAD<sup>+</sup>-dependent protein deacetylase and/or ADP-ribosyltransferase activities (Singh et al., 2018). SIRT) play critical roles in important cellular processes, and are shown to be involved in the pathogenesis of a variety of diseases, including cancer (Sebastian et al., 2012). The role of SIRT) in cancer is extremely complex and they appear to have distinct functions depending on cell contexts (Bosch-Presegue and Vaquero, 2011). The founding member of this family, the nuclear SIRT1, has been extensively studied and is linked with several health conditions including metabolic syndrome, inflammation, and cancer (Singh et al., 2018). We have earlier shown that SIRT1 is overexpressed in melanoma, and its inhibition imparts anti-proliferative responses against melanoma cells (Singh et al., 2014, Wilking et al., 2014a, Wilking et al., 2014b). One of the other well-studied sirtuins, SIRT3, is a mitochondrial sirtuin that coordinates global shifts in mitochondrial activity by deacetylating proteins involved in diverse mitochondrial functions (Su et al., 2020). SIRT3 also plays important roles in the regulation of a variety of cellular processes, including transcription, insulin secretion, and apoptosis (North and Verdin, 2004). The fact that SIRT3 can regulate several cellular processes which are critical in cancer cell proliferation makes it a promising therapeutic target for cancer management (Alhazzazi et al., 2013). In a study from our laboratory, we have demonstrated that SIRT3 is overexpressed in melanoma and its inhibition resulted in significant anti-tumor responses against melanoma *in vitro* as well as *in vivo* (George et al., 2015, Singh et al., 2021).

Recently, we discussed the potential usefulness of combined inhibition of specific sirtuins in the management of melanoma (Singh et al., 2020b). In a recent study, Nguyen et al.

demonstrated that the small molecule 4'-bromoresveratrol (4'-BR) completely inhibited the activity of both SIRT1 and SIRT3 at the 0.2 mM concentration in the deacetylation assays using FdL-1 fluorophore. Further, they identified two compound binding sites and substrate competition with NAD<sup>+</sup> as the mechanism for this inhibition (Nguyen et al., 2013). Using this compound, we have previously shown that 4'-BR treatment of multiple melanoma cell lines *in vitro* resulted in decreased cell proliferation and clonogenic survival, induction of apoptosis, and inhibition of melanoma cell migration (George et al., 2019). Moreover, as both SIRT1 and SIRT3 have been implicated in the regulation of cancer cell metabolism, their inhibition by 4'-BR treatment caused metabolic reprogramming by decreasing mitochondrial function, reducing glucose uptake and dampening NAD<sup>+</sup>/NADH ratio (George et al., 2019). In this current investigation, we determined the *in vivo* efficacy of 4'-BR against melanoma in a genetically engineered *Braf*<sup>V600E</sup>/*Pten*<sup>NULL</sup> mouse model which is known to recapitulate human melanoma's cardinal features, including lung metastases (Dankort et al., 2009). We have also analyzed potential mechanisms of action of 4'-BR against melanoma using tumors obtained from *Braf*<sup>V600E</sup>/*Pten*<sup>NULL</sup> mice and NanoString technology (PanCancer Immune Profiling Panel).

## RESULTS AND DISCUSSION

### 4'-BR significantly reduces melanoma tumor growth *in vivo* in *Braf*<sup>V600E</sup>/*Pten*<sup>NULL</sup> mice

In order to determine the translational value of combined inhibition of SIRT1 and SIRT3, in this study, we determined the *in vivo* efficacy of SIRT1 and SIRT3 dual inhibitor 4'-BR against melanomas in a genetically engineered *Braf*<sup>V600E</sup>/*Pten*<sup>NULL</sup> melanoma mouse model. This mouse model was designed to allow 4-hydroxytamoxifen (4-HT)-inducible, melanocyte-specific expression of mutant *Braf*<sup>V600E</sup> and deletion of tumor suppressor gene *Pten*, which are genetic events relevant in human melanoma. 4-HT specifically induces Cre recombinase-mutated estrogen receptor fusion transgene that is under the control of melanocyte-specific tyrosinase promoter (Tyr::CreER) (Dankort et al., 2009). Due to this, topical application of 4-HT results in development of black pigmented skin lesions that progress to malignant melanoma. In our study, pigmented spots developed 2 weeks after 4-HT treatment, at which point mice were randomly assigned to treatment groups of either vehicle or 4'-BR (5, 10, 20 or 30 mg/kg b.wt.) as described in Materials and Methods and shown in Figure 1a. The treatments were continued for 5 weeks and tumor volumes were estimated weekly.

As shown in Figure 1b, melanoma tumors in *Braf*<sup>V600E</sup>/*Pten*<sup>NULL</sup> mice were noticeably smaller after 4'-BR treatment. Images of all mice (n=6 per group) at the end of study (17 weeks) have been shown in Supplementary Figure S1. Measurement of tumor volume (Figure 1c) and tumor weight (Figure 1d) revealed that there was indeed a trend toward reduced tumor growth upon 4'-BR treatment at all tested doses in *Braf*<sup>V600E</sup>/*Pten*<sup>NULL</sup> melanomas. This difference was statistically significant at 30 mg/kg b. wt. (4'-BR) after 5 weeks, therefore, tumor tissues derived from this group and control were used subsequently for molecular analyses. Further, we found no significant change in body weight after treatment (Figure 1e) and there were no noticeable adverse effects of 4'-BR treatment at the tested doses. A previous study has demonstrated that 4'-BR inhibited the activity of SIRT1

and SIRT3, by binding to the allosteric site and substrate competition with NAD<sup>+</sup> (Nguyen et al., 2013). We determined the expression of these sirtuins in 4-HT-induced mouse melanomas and verify if 4'-BR modulated their expression in these tumors by performing a quantitative immunodetection analysis using ProteinSimple. Our results suggested that both SIRT1 and SIRT3 are expressed in *Braf*<sup>V600E</sup>/*Pten*<sup>NULL</sup> tumors validating the target expression. Furthermore, we found no significant change in protein levels of SIRT1 and SIRT3 after 4'-BR treatment, suggesting that 4'-BR does not affect the protein expression of these sirtuins (Supplementary Figure S2), and the observed effects could be due to the inhibition of their activity.

Since 4'-BR has not been investigated in *in vivo* cancer models including melanoma, these are important and promising pre-clinical observations in *Braf*<sup>V600E</sup>/*Pten*<sup>NULL</sup> melanoma mouse model, which is an excellent model for pre-clinical evaluation of anti-melanoma agents due to its close resemblance with human melanoma (Marsh Durban et al., 2013, Vitiello et al., 2019).

#### **4'-BR treatment modulates key markers of melanoma progression in *Braf*<sup>V600E</sup>/*Pten*<sup>NULL</sup> mice**

Next, tumor samples obtained from the 30 mg/kg and control groups were analyzed for Ki67 and PCNA (proliferating cell nuclear antigen) as biomarkers of cell proliferation (Li et al., 2015). Additionally, we used survivin as a biomarker of cell survival, as it prevents programmed cell death and is shown to be associated with melanoma progression (McKenzie and Grossman, 2012). As shown in Figure 2a, 4'-BR treatment significantly reduced the percent of Ki67-positive cells in tumors, indicating decreased proliferative indices in this group. Further, our results showed a marked reduction in PCNA and survivin both at mRNA and protein levels (Figure 2b). Furthermore, we analyzed growth factor signaling markers insulin-like growth factor 1 (IGF1) a tumor-promoting growth factor, and insulin-like growth factor-binding protein 5 (IGFBP5) a tumor suppressor protein. We observed decreased *Igf1* and increased *Igfbp5* in response to 4'-BR treatment at mRNA levels as well as an increase in IGFBP5 at protein level (Figure 2b). IGF1 has been shown to promote melanoma progression by increasing proliferation, tumor cell mobility and dissemination, maintaining stemness features crucial for the immune escape, chemoresistance, and tumorigenicity (Le Coz et al., 2016). Further, IGFBP5 has been shown to function as an important tumor suppressor gene in melanoma tumorigenicity and metastasis using both *in vitro* and *in vivo* experiments (Wang et al., 2015). Thus, the observed decrease in Ki67, PCNA, survivin and IGF1, as well as increase in IGFBP5 by 4'-BR treatment, demonstrate anti-melanoma potential of this dual SIRT1 and SIRT3 inhibitor.

Since melanoma has been linked with dysregulated oxidative stress with deteriorated cell functioning at the mitochondrial level (Bisevac et al., 2018, Denat et al., 2014), we assessed the effects of 4'-BR treatment on selected markers of oxidative stress, viz. nuclear factor-erythroid 2 related factor (NRF2) and Kelch-like ECH Associated Protein 1 (KEAP1). Using RT-qPCR, we found that 4'-BR treatment significantly up-regulated *Keap1* compared to a slight decrease in *Nrf2*, resulting in a significant decrease in the ratio of *Nrf2/Keap1*

(Figure 2c). NRF2 is known to play an important role in cell survival and defense against endogenous/exogenous stresses, and generally, its overexpression in cancer cells enhances the expression of cytoprotective genes, resulting in increased cell proliferation and inhibition of apoptosis (Sajadimajd and Khazaei, 2018). KEAP1, a negative regulator of NRF2, is known to bind and restrict NRF2 activation. Recently, some reports have shown that NRF2 expression in melanoma is related to invasion, thereby worsening melanoma-specific survival (Hintsala et al., 2016).

Overall, our data demonstrate the ability of 4'-BR to exert anti-proliferative and anti-tumorigenic effects in a human-relevant melanoma mouse model with significant modulations in markers of cell proliferation, cell survival, tumor growth and oxidative stress.

#### 4'-BR modulates genes associated with cancer immune pathways

Given that *Brat<sup>V600E</sup>/Pten<sup>NULL</sup>* is an inducible melanoma mouse model with an active immune system, it is a powerful tool to study the immune modulations in response to therapy. As sirtuins are linked to immunomodulation, and melanoma is an immunologically "hot" cancer, we performed differential gene expression analysis using high throughput multiplex analysis via NanoString nCounter PanCancer Immune Profiling panel, which analyzes 770 genes related to cancer-immune pathways (cancer progression, chemokines and cytokines and their receptors, and innate and adaptive immune response). nSolver software was used to analyze the data and a heat map was generated to show differential expression of 770 genes (Figure 3a). Further, using a fold cut-off of 2 and p-value <0.05, we observed that 4'-BR significantly modulated the expression of multiple genes as shown via volcano plot (Figure 3a). Moreover, several cancer immune pathways were significantly downregulated by 4'-BR treatment, while senescence and T-cell functions were significantly upregulated (Figure 3b). Overall, this high throughput gene expression analysis suggested that 4'-BR treatment strongly favored systemic antitumor immunity, resulting in inhibition of tumor growth in mice.

At a more granular level, we found that 49 genes were significantly (fold cut-off of 2 and p-value <0.05) affected by 4'-BR treatment, the associations and interactions of which were further studied by performing network analysis. As shown in Figure 4a, found that a majority of the 49 genes modulated by 4'-BR treatment were highly interconnected. Interestingly, out of these 49 genes, 41 were downregulated, while only 8 were upregulated after 4'-BR treatment (indicated with dashed outlines in Figures 4a and 4b). Three genes out of the 49 did not show evidence of interaction within the other genes in the network: *Colec12*, *Rae1c*, and *Prg2*. However, *Itgam* (integrin subunit alpha M) demonstrated to have the most interactions (25 interactions with other genes), which is not unexpected as it is a member of the integrin family of transmembrane adhesion molecules that facilitate cell-cell and cell-extracellular matrix attachments. On the other hand, *Sigirr*, *Fap*, and *Jam3* had the least interactions (1 interaction each). Overall, network analyses of the genes affected by 4'-BR treatment revealed that 18 genes were involved in innate/adaptive immune functions, 14 genes were associated with cancer progression/adhesion/apoptosis, 9 genes had basic/immune cell functions, and 8 genes which were chemokines/cytokines (Figure 4a).

Furthermore, genes that had evidence of roles in melanoma were analyzed using network visualization (Figure 4b). Out of the 49 total genes that were affected by 4'-BR treatment, 30 genes have been associated with melanoma. A literature analysis of the 30 genes reported to be associated with melanoma and significantly affected by 4'-BR treatment in *Braf*<sup>V600E</sup>/*Pten*<sup>NULL</sup> mice has been detailed in Table 1. Interestingly, in our network analysis, all the 30 genes showed evidence of at least one interaction with each other. *Fn1* had the most interactions (14 interactions with other genes) while *Il21r*, *Fap*, and *Jam3* had the least interactions (1 each). Importantly, in a recent study, *Fn1* (Fibronectin 1) was shown to promote melanoma proliferation and metastasis by inhibiting apoptosis and regulating epithelial to mesenchymal transition (EMT) (Li et al., 2019), suggesting it may be directly affected by 4'-BR treatment. Of these 30 melanoma-involved genes, 23 were downregulated and 7 were upregulated after 4'-BR treatment. From the 23 downregulated genes, 21 have been shown to support melanoma progression and 2 to inhibit it. Of the 7 upregulated genes, 6 genes are known to inhibit melanoma, and 1 has been associated with melanoma development (Figure 4b).

A review of available literature revealed that 10 of these downregulated genes (*Ccr1*, *Itgam*, *S100a8*, *C1qb*, *F13a1*, *Il1b*, *Fap*, *Col3a1*, *Angpt2*, and *Spp1*) were associated with increased risk of melanoma and their expression was dysregulated in melanoma (detailed in Table 1). Additionally, their expression has been correlated with poor survival in melanoma patients, suggesting they could be explored as melanoma markers. Similarly, 6 genes (*Fn1*, *Jam3*, *Thbd*, *Angpt1*, *Ptgs2*, and *Ccr5*) downregulated following 4'-BR treatment were involved in promoting tumorigenesis, cell migration and invasion, and epithelial to EMT. Furthermore, 5 downregulated genes (*Nlrp3*, *Cd33*, *Serp1g1*, *Tlr2*, and *Gpr183*) have been reported to play immune-related roles, which contribute to melanoma progression. On the other hand, two genes (*IL21R* and *OSM*) downregulated after 4'-BR treatment have been reported to inhibit melanoma progression by suppressing tumorigenesis as well as blocking cell proliferation and invasion. Interestingly, all 7 genes that were upregulated after 4'-BR treatment (*Il12rb2*, *Xcl1*, *Ccl1*, *Zap70*, *Rorc*, *Tnfsf10*, and *Ccl19*) have been reported to inhibit melanoma progression, which is consistent with the anti-melanoma effects of 4'-BR. Specifically, 4 upregulated genes (*Xcl1*, *Ccl1*, *Zap70*, and *Ccl19*) share immune-related functions which have anti-tumor effects and thus are correlated with good prognosis. The remaining 3 upregulated genes (*Il12rb2*, *Rorc*, and *Tnfsf10*) are tumor suppressor genes which are associated with prolonged survival of melanoma patients and even could be potential candidates for treatments against melanoma. Overall, our findings support the antiproliferative effects of 4'-BR and suggest that this response may occur via modulation of important tumor suppressor pathways, immune responses, and reductions in cell proliferation and invasion pathways.

#### 4'-BR modulates protein expression of immune and inflammatory markers

Considering that melanoma has been classified as an immunogenic malignancy (Franklin et al., 2017) together with the immune- and inflammatory-related roles that SIRT1 and SIRT3 carry out (Vachharajani et al., 2016), we determined the potential immunomodulatory effects after 4'-BR treatment in melanoma tumors. Likewise, to confirm our Nanostring transcriptomic data on immunomodulatory activities of 4'-BR, we performed IHC analysis

for certain immune and inflammatory markers obtained from Nanostring analysis. Using melanoma tumors from control and 4'-BR at 30 mg/kg b. wt. dose groups (n=6), we determined the potential differences in protein levels of program death-ligand 1 (PDL-1), interleukin-1 beta (IL-1 $\beta$ ), and NOD-like receptor family pyrin domain containing 3 (NLRP3).

PDL-1, found in cancerous or infiltrating immune cells, is a ligand of the programmed death receptor 1 (PD-1), which together can provide cells the ability to evade the immune system (Kythreotou et al., 2018). In our Nanostring analysis, we found that the gene that encodes for PD-L1 (CD274) was slightly increased in 4'-BR treated group, although the change was not statistically significant. In our IHC analysis, we observed no significant changes in PDL-1 expression in 4'-BR when compared to control group (Figure 4c). It is possible that this slight/no change in PD-L1 levels in both assays may be due to the complexity of using PD-L1 as a biomarker, since it has been shown that PD-L1 levels widely vary across tumor tissues (Patel and Kurzrock, 2015, Schats et al., 2017).

To further evaluate the effects of 4'-BR treatment on inflammatory markers, we used IHC to confirm our results from Nanostring analysis on selected statistically significant downregulated genes after 4'-BR treatment, IL-1 $\beta$  and NLRP3. IL-1 $\beta$  is a proinflammatory cytokine that can be produced by malignant cells to increase their invasiveness (Jiang et al., 2015). NLRP3 is an inflammasome that is constitutively activated in melanoma cells and when it is inhibited this leads to decreased melanoma invasion and metastasis *in vitro* and *in vivo* (Lee et al., 2019). Interestingly, it has been shown that melanoma cells activate NLRP3 which induces IL-1 $\beta$  secretion (Lee et al., 2019, Zhai et al., 2017). Accordingly, increased levels of IL-1 $\beta$  and NLRP3 have been associated with melanoma development and progression (da Silva et al., 2016, Zhai et al., 2017). Using IHC, for both IL-1 $\beta$  and NLRP3, our results showed a clear reduction of protein levels in 4'-BR when compared to control group (Figure 4c). Altogether, these experiments provide preliminary data in terms of the immunomodulatory effects that 4'-BR treatment imparts in melanoma tumors.

#### 4'-BR treatment reduces melanoma metastasis in *Braf*<sup>V600E</sup>/*Pten*<sup>NULL</sup> mice

The *Braf*<sup>V600E</sup>/*Pten*<sup>NULL</sup> mouse model is an excellent model as it has a high rate of metastatic disease in a manner that recapitulates the clinical course of melanoma in humans, which provides an opportunity for studying mechanisms of melanomagenesis, melanoma progression and metastasis (Dankort et al., 2009). To explore the effects of 4'-BR on melanoma metastasis, we analyzed the resected lungs from the mice at the termination of the experiment. Visually, we observed a marked decrease in lung metastasis at the end of study (17 weeks) as shown in Figures 5a. Additionally, using melanoma tumors, we also found a significant decrease in vimentin at both protein and mRNA levels following 4'-BR treatment (Figure 5b). This is an interesting data, as vimentin has been reported to be a metastatic indicator in melanoma and its higher expression in primary human melanoma tissues may indicate patients with high risk of hematogenous metastasis (Li et al., 2010).

To further explore the mechanisms behind this reduction in metastatic potential, we validated several genes associated with melanoma progression and metastasis obtained from our network analysis of NanoString data. Using primary melanoma tumors obtained



from 4'-BR treatment group, our RT-qPCR analysis showed significant downregulation of several genes promoting melanoma progression and metastasis such as *S1008a*, *Thbd*, *Il1b*, *Fap*, *Angpt1*, *Angpt2*, *Ptgs2*, *Fn1*, *Jam3*, and *Spp1* (Figure 5c). We also validated two tumor suppressor genes *Zap70* and *Rorc* which have been shown to inhibit melanoma metastasis. *Zap70* showed a significant increase, while *Rorc* showed a marked but non-significant increase in 4'-BR treated tumors (Figure 5d). Further, some of the significantly modulated genes obtained from NanoString data analysis were found either with no change or not significant in our validation by RT-qPCR such as *Osm*, *Il21r*, *Ccr5* and *Gpr183* (Supplementary Figure S3). Together, these results strongly support the anti-metastatic potential of 4'-BR treatment in *Braf<sup>V600E</sup>/Pten<sup>NULL</sup>* melanoma tumors.

Collectively, our investigation demonstrates the ability of 4'-BR to inhibit melanoma *in vivo* with no noticeable adverse effects in a human-relevant melanoma mouse model. Additionally, 4'-BR was able to visibly reduce melanoma metastasis to the lungs, which was associated with reductions in metastasis-related genes via RT-qPCR. These results in combination with high-throughput multiplex analysis using Nanostring Mouse PanCancer Immune Profiling Panel suggest that 4'-BR, a dual SIRT-1 and SIRT-3 inhibitor, may be a promising anti-melanoma agent with anti-metastatic and immunomodulatory effects, warranting further investigations including clinical studies.

## MATERIALS AND METHODS

### Animals and materials

Animal experiments were approved by the University of Wisconsin (UW) Institutional Animal Care and Use Committee. Genetically engineered *Braf<sup>tm1Mmcm</sup> Pten<sup>tm1Hwu</sup> Tg(Tyrcre/ERT2)13Bos/BosJ* mice (8-9 weeks old) were purchased from The Jackson Laboratory (Stock Number: 012328; Bar Harbor, ME). Mice were maintained under defined conditions and experiments were performed in accordance with the NIH Guide for the Care and Use of Laboratory Animals and institutional guidelines. Mice were acclimatized for at least one week before start of the experiment. 5-([E]-2-[4-bromophenyl]vinyl)benzene-1,3-diol (4'-BR) was obtained from Aobious (Gloucester, MA). 4-hydroxytamoxifen (4-HT) was purchased from Cayman Chemical (Ann Arbor, MI).

### *In vivo* melanoma development and treatments

Localized melanoma tumors were induced on the back skin of *Braf<sup>V600E</sup>/Pten<sup>NULL</sup>* mice as described previously (Dankort et al., 2009). Briefly, dorsal hair was removed and 2  $\mu$ L of 5 mmol/L 4-HT dissolved in dimethyl sulfoxide (DMSO; Sigma-Aldrich, St. Louis, MO) was topically applied in four discrete spots on 10-week-old mice for three consecutive days. Mice were monitored for overall health and the presence of cutaneous malignant melanoma. As shown in Figure 1a, after 2 weeks mice harboring established melanoma were randomly divided in 5 groups (n=6, 3 male and 3 female) and treated with 4'-BR (5, 10, 20 and 30 mg/kg b.wt.; intraperitoneal (i.p.); 3d/week for 5 weeks) or an equivalent volume of vehicle (50% DMSO + 50% polyethylene glycol (PEG)).

### **Tumor analysis and lung metastasis**

During the study, mice were monitored for melanoma development. Tumor growth was determined using digital calipers, and tumor sizes were represented as mean $\pm$ SEM (n=6). At the termination of the experiment, tumors were measured using a digital caliper and tumor volume was calculated using the formula  $0.5 \times \text{length} \times \text{width}^2$ . Further, at the termination of experiments tumors were excised, and weighed before being divided into either formalin (for immunohistochemistry (IHC) analysis) or snap-frozen (for protein/RNA analysis). Lungs were harvested and fixed in Fekete's solution (Overwijk and Restifo, 2001) to visualize metastasis. All other analyses related to metastatic markers were performed using primary melanoma tumors obtained from 4'-BR treatment and control groups. Statistical significance was determined via t-test using GraphPad Prism software.

### **Quantitative immunodetection analysis by ProteinSimple**

Quantitative immunodetection analysis was done on protein lysates per manufacturer's protocol (see Supplementary Materials and Methods). Briefly, protein from tumor tissues were isolated in 1X RIPA lysis buffer (Millipore, Burlington, MA) with Protease Inhibitor Cocktail (Thermo Scientific, Waltham, MA) and PMSF (Amresco, Solon, OH), and quantified using Pierce BCA Protein assay kit. Protein expression was measured with automated protein capillary electrophoresis using a ProteinSimple Wes instrument (ProteinSimple, San Jose, CA). The assay was optimized for the targets of interest and tissue samples (Supplementary Figure S4 and Supplementary Figure S5, Supplementary Table S1).

### **Immunohistochemistry (IHC)**

After excision, tumors were fixed in 10% formalin for 48 hours before rinsing and stored short-term in 70% ethanol. After fixation, tissues were embedded in paraffin, sectioned, and mounted on slides at the UW Translational Research Initiatives in Pathology (TRIP) lab. IHC analysis was performed as described recently (Singh et al., 2020a) utilizing ABC-HRP reagent (Vector Labs, Burlingame, CA), Vector Red chromogen and hematoxylin per manufacturer's protocol. The primary antibodies used in IHC analysis are detailed in Supplementary Table S2. Imaging and analysis were performed per details in Supplementary Materials and Methods. Statistical analysis was performed using two-tailed unpaired Student's t-test using GraphPad Prism software.

### **RNA isolation and reverse transcription-quantitative real-time PCR (RT-qPCR)**

RNA was isolated using the RNeasy Plus kit and quantified using the BioTek Synergy H1 multimode plate reader. RNA from 6 mice were pooled in each group to make 3 groupings of RNA per group for further analysis. cDNA was made using M-MLV reverse transcriptase and oligo dT primers. RT-qPCR analysis was performed using QuantStudio 3 with SYBR Premix Ex Taq II with cDNA and primers (Supplementary Table S3). Relative mRNA levels were analyzed using ACTB as endogenous control and  $\Delta\Delta$ CT algorithm. Statistical significance was determined via multiple t-tests using the Holm-Sidak method to correct for multiple comparisons using GraphPad Prism software.

## NanoString PanCancer Immune Profiling Panel analysis

RNA from control and 4'-BR-treated (30 mg/kg b. wt.) mice ( $n = 6$ ) were used to determine the expression of 770 genes (730 immune genes and 40 housekeeping genes) via the Mouse PanCancer Immune Profiling Panel using nCounter platform in the NanoString Technologies laboratories. nSolver software with an advanced analysis module (NanoString Technologies, Seattle, WA) was used for quality control, normalization, differential gene expression, and functional pathways score analyses in accordance with guidance provided by Nanostring. Principle component analysis (PCA) was performed to assess sample grouping (Figure S6). The expression levels of each gene were normalized to housekeeping genes. Fold changes greater than 2-fold upregulation or downregulation with p-values  $<0.05$  between the two groups were considered significant. The heat map for differentially expressed genes in 4'-BR (30 mg/kg b. wt.) group compared to control group was plotted and analyzed using nSolver software.

## Network analyses

Network analyses were carried out as described previously with a few modifications (Bates et al., 2019). Genes with significant fold changes ( $\geq 2$ ) were considered for network analysis. The STRING database version 11.0 (<https://string-db.org>) was used for the prediction of gene interactions, based on information from previous publications (Szkarczyk et al., 2019). Since the number of genes was relatively small (49 significantly altered genes), the minimum required interaction score was set at a confidence level of 0.4. Using STRING, clusters were visualized by selecting the Markov Cluster (MCL) algorithm as part of the analysis, with an inflation parameter of 1.5. Furthermore, network edges (lines that connect the genes with one another) were defined in STRING as the molecular action between genes, to visualize the type and effect of mode of action. Afterward, gene networks were transferred to Cytoscape version 3.8 for visualization (Shannon et al., 2003). Nodes represent genes of interest while lines or edges correspond to interactions between those genes. Visualizations were refined using Adobe Illustrator 2019.

## Supplementary Material

Refer to Web version on PubMed Central for supplementary material.

## ACKNOWLEDGEMENTS

We thank Ms. Deeba Amiri and Mr. Brian Su for their technical help with immunohistochemistry and Cytoscape network analyses, respectively. This work was partially supported by funding from the NIH (R01AR059130 and R01CA176748 to NA), and the Department of Veterans Affairs (VA Merit Review Awards I01CX001441 and I101BX004221-01; and a Research Career Scientist Award IK6BX003780 to NA). In addition, we acknowledge the support from the UW Skin Diseases Research Center (SDRC; NIH/NAIAMS P30AR066524) as well as the UW Institute for Clinical and Translational Research (NIH/NCATS CTSA award UL1TR002373). Finally, we thank the UW Translational Research Initiatives in Pathology laboratory (TRIP), supported by the UW Department of Pathology and Laboratory Medicine, UWCCC (P30 CA014520) and the Office of The Director- NIH (S10 OD023526) for use of its facilities and services.

## DATA AVAILABILITY

Datasets related to this article (NanoString PanCancer Immune Profiling Panel) can be found at NCBI's Gene Expression Omnibus (Edgar et al., 2002) and are accessible through GEO Series accession number GSE168564.

(<https://www.ncbi.nlm.nih.gov/geo/query/acc.cgi?acc=GSE168564>).

## REFERENCES

- Airoidi I, Di Carlo E, Cocco C, Taverniti G, D'Antuono T, Ognio E, et al. Endogenous IL-12 triggers an antiangiogenic program in melanoma cells. *Proc Natl Acad Sci U S A* 2007;104(10):3996–4001. [PubMed: 17360466]
- Alhazzazi TY, Kamarajan P, Verdin E, Kapila YL. Sirtuin-3 (SIRT3) and the Hallmarks of Cancer. *Genes & cancer* 2013;4(3-4):164–71. [PubMed: 24020007]
- Arcangeli ML, Frontera V, Bardin F, Thomassin J, Chetaille B, Adams S, et al. The Junctional Adhesion Molecule-B regulates JAM-C-dependent melanoma cell metastasis. *FEBS Lett* 2012;586(22):4046–51. [PubMed: 23068611]
- Azimi A, Pernemalm M, Frostvik Stolt M, Hansson J, Lehtio J, Egyhazi Brage S, et al. Proteomics analysis of melanoma metastases: association between S100A13 expression and chemotherapy resistance. *British journal of cancer* 2014;110(10):2489–95. [PubMed: 24722184]
- Bates MA, Benninghoff AD, Gilley KN, Holian A, Harkema JR, Pestka JJ. Mapping of Dynamic Transcriptome Changes Associated With Silica-Triggered Autoimmune Pathogenesis in the Lupus-Prone NZBWF1 Mouse. *Front Immunol* 2019;10:632. [PubMed: 30984195]
- Bisevac JP, Djukic M, Stanojevic I, Stevanovic I, Mijuskovic Z, Djuric A, et al. Association Between Oxidative Stress and Melanoma Progression. *J Med Biochem* 2018;37(1):12–20. [PubMed: 30581337]
- Blattner C, Fleming V, Weber R, Himmelhan B, Altevogt P, Gebhardt C, et al. CCR5(+) Myeloid-Derived Suppressor Cells Are Enriched and Activated in Melanoma Lesions. *Cancer Res* 2018;78(1):157–67. [PubMed: 29089297]
- Bogunovic D, O'Neill DW, Belitskaya-Levy I, Vacic V, Yu YL, Adams S, et al. Immune profile and mitotic index of metastatic melanoma lesions enhance clinical staging in predicting patient survival. *Proc Natl Acad Sci U S A* 2009;106(48):20429–34. [PubMed: 19915147]
- Bosch-Presegue L, Vaquero A. The dual role of sirtuins in cancer. *Genes & cancer* 2011;2(6):648–62. [PubMed: 21941620]
- Botelho NK, Tschumi BO, Hubbell JA, Swartz MA, Donda A, Romero P. Combination of Synthetic Long Peptides and XCL1 Fusion Proteins Results in Superior Tumor Control. *Front Immunol* 2019;10:294. [PubMed: 30863405]
- Brozyna AA, Jozwicki W, Skobowiat C, Jetten A, Slominski AT. RORalpha and RORgamma expression inversely correlates with human melanoma progression. *Oncotarget* 2016;7(39):63261–82. [PubMed: 27542227]
- Chen Y, Sumardika IW, Tomonobu N, Winarsa Ruma IM, Kinoshita R, Kondo E, et al. Melanoma cell adhesion molecule is the driving force behind the dissemination of melanoma upon S100A8/A9 binding in the original skin lesion. *Cancer Lett* 2019;452:178–90. [PubMed: 30904617]
- da Silva WC, Oshiro TM, de Sa DC, Franco DD, Festa Neto C, Pontillo A. Genotyping and differential expression analysis of inflammasome genes in sporadic malignant melanoma reveal novel contribution of CARD8, IL1B and IL18 in melanoma susceptibility and progression. *Cancer Genet* 2016;209(10):474–80. [PubMed: 27810076]
- Dankort D, Curley DP, Cartlidge RA, Nelson B, Karnezis AN, Damsky WE Jr., et al. Braf(V600E) cooperates with Pten loss to induce metastatic melanoma. *Nat Genet* 2009;41(5):544–52. [PubMed: 19282848]

- Davis ID, Skak K, Smyth MJ, Kristjansen PE, Miller DM, Sivakumar PV. Interleukin-21 signaling: functions in cancer and autoimmunity. *Clin Cancer Res* 2007;13(23):6926–32. [PubMed: 18056166]
- de Andrade LF, Lu Y, Luoma A, Ito Y, Pan D, Pyrdol JW, et al. Discovery of specialized NK cell populations infiltrating human melanoma metastases. *JCI Insight* 2019;4(23).
- de Oliveira Ada S, Yang L, Echevarria-Lima J, Monteiro RQ, Rezaie AR. Thrombomodulin modulates cell migration in human melanoma cell lines. *Melanoma Res* 2014;24(1):11–9. [PubMed: 24366193]
- de Wit NJ, Rijntjes J, Diepstra JH, van Kuppevelt TH, Weidle UH, Ruiter DJ, et al. Analysis of differential gene expression in human melanocytic tumour lesions by custom made oligonucleotide arrays. *British journal of cancer* 2005;92(12):2249–61. [PubMed: 15900300]
- Denat L, Kadekaro AL, Marrot L, Leachman SA, Abdel-Malek ZA. Melanocytes as instigators and victims of oxidative stress. *The Journal of investigative dermatology* 2014;134(6):1512–8. [PubMed: 24573173]
- Eberle J. Countering TRAIL Resistance in Melanoma. *Cancers (Basel)* 2019;11(5).
- Edgar R, Domrachev M, Lash AE. Gene Expression Omnibus: NCBI gene expression and hybridization array data repository. *Nucleic Acids Res* 2002;30(1):207–10. [PubMed: 11752295]
- Ercolano G, De Cicco P, Rubino V, Terrazzano G, Ruggiero G, Carriero R, et al. Knockdown of PTGS2 by CRISPR/CAS9 System Designates a New Potential Gene Target for Melanoma Treatment. *Front Pharmacol* 2019;10:1456. [PubMed: 31920649]
- Fan J, Lv Z, Yang G, Liao TT, Xu J, Wu F, et al. Retinoic Acid Receptor-Related Orphan Receptors: Critical Roles in Tumorigenesis. *Front Immunol* 2018;9:1187. [PubMed: 29904382]
- Flaherty KT, Infante JR, Daud A, Gonzalez R, Kefford RF, Sosman J, et al. Combined BRAF and MEK inhibition in melanoma with BRAF V600 mutations. *The New England journal of medicine* 2012;367(18):1694–703. [PubMed: 23020132]
- Franklin C, Livingstone E, Roesch A, Schilling B, Schadendorf D. Immunotherapy in melanoma: Recent advances and future directions. *Eur J Surg Oncol* 2017;43(3):604–11. [PubMed: 27769635]
- Furuta J, Kaneda A, Umebayashi Y, Otsuka F, Sugimura T, Ushijima T. Silencing of the thrombomodulin gene in human malignant melanoma. *Melanoma Res* 2005;15(1):15–20. [PubMed: 15714116]
- Gardizi M, Kurschat C, Riese A, Hahn M, Krieg T, Mauch C, et al. A decreased ratio between serum levels of the antagonistic angiopoietins 1 and 2 indicates tumour progression of malignant melanoma. *Arch Dermatol Res* 2012;304(5):397–400. [PubMed: 22410864]
- George J, Nihal M, Singh CK, Ahmad N. 4'-Bromo-resveratrol, a dual Sirtuin-1 and Sirtuin-3 inhibitor, inhibits melanoma cell growth through mitochondrial metabolic reprogramming. *Mol Carcinog* 2019;58(10):1876–85. [PubMed: 31292999]
- George J, Nihal M, Singh CK, Zhong W, Liu X, Ahmad N. Pro-proliferative function of mitochondrial sirtuin deacetylase SIRT3 in human melanoma. *J Invest Dermatol*, 2016;136:809–818. [PubMed: 26743598]
- Ghislin S, Obino D, Middendorp S, Boggetto N, Alcaide-Loridan C, Deshayes F. Junctional adhesion molecules are required for melanoma cell lines transendothelial migration in vitro. *Pigment Cell Melanoma Res* 2011;24(3):504–11. [PubMed: 21466663]
- Gonzalez FE, Ortiz C, Reyes M, Dutzan N, Patel V, Pereda C, et al. Melanoma cell lysate induces CCR7 expression and in vivo migration to draining lymph nodes of therapeutic human dendritic cells. *Immunology* 2014;142(3):396–405. [PubMed: 24673602]
- Gowrishankar K, Snoyman S, Pupo GM, Becker TM, Kefford RF, Rizos H. Acquired resistance to BRAF inhibition can confer cross-resistance to combined BRAF/MEK inhibition. *The Journal of investigative dermatology* 2012;132(7):1850–9. [PubMed: 22437314]
- Hill R, Kalathur RK, Colaco L, Brandao R, Ugurel S, Futschik M, et al. TRIB2 as a biomarker for diagnosis and progression of melanoma. *Carcinogenesis* 2015;36(4):469–77. [PubMed: 25586991]
- Hintsala HR, Jokinen E, Haapasaari KM, Moza M, Ristimaki A, Soini Y, et al. Nrf2/Keap1 Pathway and Expression of Oxidative Stress Lesions 8-hydroxy-2'-deoxyguanosine and Nitrotyrosine in Melanoma. *Anticancer Res* 2016;36(4):1497–506. [PubMed: 27069125]

- Hsu YY, Shi GY, Kuo CH, Liu SL, Wu CM, Ma CY, et al. Thrombomodulin is an ezrin-interacting protein that controls epithelial morphology and promotes collective cell migration. *FASEB J* 2012;26(8):3440–52. [PubMed: 22593542]
- Huang R, Andersen LMK, Rofstad EK. Metastatic pathway and the microvascular and physicochemical microenvironments of human melanoma xenografts. *J Transl Med* 2017;15(1):203. [PubMed: 29017512]
- Huang S, Zhang Y, Wang L, Liu W, Xiao L, Lin Q, et al. Improved melanoma suppression with target-delivered TRAIL and Paclitaxel by a multifunctional nanocarrier. *J Control Release* 2020;325:10–24. [PubMed: 32251770]
- Jenkins RW, Fisher DE. Treatment of Advanced Melanoma in 2020 and Beyond. *J Invest Dermatol*, 2021;141:23–31. [PubMed: 32268150]
- Jiang H, Gebhardt C, Umansky L, Beckhove P, Schulze TJ, Utikal J, et al. Elevated chronic inflammatory factors and myeloid-derived suppressor cells indicate poor prognosis in advanced melanoma patients. *Int J Cancer* 2015;136(10):2352–60. [PubMed: 25353097]
- Jordan KR, Amaria RN, Ramirez O, Callihan EB, Gao D, Borakove M, et al. Myeloid-derived suppressor cells are associated with disease progression and decreased overall survival in advanced-stage melanoma patients. *Cancer Immunol Immunother* 2013;62(11):1711–22. [PubMed: 24072401]
- Klarquist J, Tobin K, Farhangi Oskuei P, Henning SW, Fernandez MF, Dellacecca ER, et al. Ccl22 Diverts T Regulatory Cells and Controls the Growth of Melanoma. *Cancer Res* 2016;76(21):6230–40. [PubMed: 27634754]
- Kong LY, Wei J, Sharma AK, Barr J, Abou-Ghazal MK, Fokt I, et al. A novel phosphorylated STAT3 inhibitor enhances T cell cytotoxicity against melanoma through inhibition of regulatory T cells. *Cancer Immunol Immunother* 2009;58(7):1023–32. [PubMed: 19002459]
- Koroknai V, Szasz I, Hernandez-Vargas H, Fernandez-Jimenez N, Cuenin C, Herceg Z, et al. DNA hypermethylation is associated with invasive phenotype of malignant melanoma. *Exp Dermatol* 2020;29(1):39–50. [PubMed: 31602702]
- Kythreotou A, Siddique A, Mauri FA, Bower M, Pinato DJ. Pd-L1. *J Clin Pathol* 2018;71(3):189–94. [PubMed: 29097600]
- Lazar-Molnar E, Hegyesi H, Toth S, Falus A. Autocrine and paracrine regulation by cytokines and growth factors in melanoma. *Cytokine* 2000;12(6):547–54. [PubMed: 10843728]
- Le Coz V, Zhu C, Devocelle A, Vazquez A, Boucheix C, Azzi S, et al. IGF-1 contributes to the expansion of melanoma-initiating cells through an epithelial-mesenchymal transition process. *Oncotarget* 2016;7(50):82511–27. [PubMed: 27764776]
- Lee HE, Lee JY, Yang G, Kang HC, Cho YY, Lee HS, et al. Inhibition of NLRP3 inflammasome in tumor microenvironment leads to suppression of metastatic potential of cancer cells. *Sci Rep* 2019;9(1):12277. [PubMed: 31439870]
- Lenci RE, Rachakonda PS, Kubarenko AV, Weber AN, Brandt A, Gast A, et al. Integrin genes and susceptibility to human melanoma. *Mutagenesis* 2012;27(3):367–73. [PubMed: 22189006]
- Li B, Shen W, Peng H, Li Y, Chen F, Zheng L, et al. Fibronectin 1 promotes melanoma proliferation and metastasis by inhibiting apoptosis and regulating EMT. *Onco Targets Ther* 2019;12:3207–21. [PubMed: 31118673]
- Li LT, Jiang G, Chen Q, Zheng JN. Ki67 is a promising molecular target in the diagnosis of cancer (review). *Mol Med Rep* 2015;11(3):1566–72. [PubMed: 25384676]
- Li M, Zhang B, Sun B, Wang X, Ban X, Sun T, et al. A novel function for vimentin: the potential biomarker for predicting melanoma hematogenous metastasis. *J Exp Clin Cancer Res* 2010;29:109. [PubMed: 20701774]
- Liu J, Wang C, Ma X, Tian Y, Wang C, Fu Y, et al. High expression of CCR5 in melanoma enhances epithelial-mesenchymal transition and metastasis via TGFbeta1. *J Pathol* 2019;247(4):481–93. [PubMed: 30474221]
- Luo Y, Robinson S, Fujita J, Siconolfi L, Magidson J, Edwards CK, et al. Transcriptome profiling of whole blood cells identifies PLEK2 and C1QB in human melanoma. *PLoS One* 2011;6(6):e20971. [PubMed: 21698244]

- Marsh Durban V, Deuker MM, Bosenberg MW, Phillips W, McMahon M. Differential AKT dependency displayed by mouse models of BRAFV600E-initiated melanoma. *J Clin Invest* 2013;123(12):5104–18. [PubMed: 24200692]
- Martins WK, Esteves GH, Almeida OM, Rezze GG, Landman G, Marques SM, et al. Gene network analyses point to the importance of human tissue kallikreins in melanoma progression. *BMC Med Genomics* 2011;4:76. [PubMed: 22032772]
- Mauldin IS, Wang E, Deacon DH, Olson WC, Bao Y, Slingluff CL Jr. TLR2/6 agonists and interferon-gamma induce human melanoma cells to produce CXCL10. *Int J Cancer* 2015;137(6):1386–96. [PubMed: 25765738]
- McKenzie JA, Grossman D. Role of the apoptotic and mitotic regulator survivin in melanoma. *Anticancer Res* 2012;32(2):397–404. [PubMed: 22287725]
- Messina JL, Fenstermacher DA, Eschrich S, Qu X, Berglund AE, Lloyd MC, et al. 12-Chemokine gene signature identifies lymph node-like structures in melanoma: potential for patient selection for immunotherapy? *Sci Rep* 2012;2:765. [PubMed: 23097687]
- Michael IP, Orebrand M, Lima M, Pereira B, Volpert O, Quaggin SE, et al. Angiopoietin-1 deficiency increases tumor metastasis in mice. *BMC cancer* 2017;17(1):539. [PubMed: 28800750]
- Minisini AM, Pascoletti G, Intersimone D, Poletto E, Driol P, Spizzo R, et al. Expression of thymidine phosphorylase and cyclooxygenase-2 in melanoma. *Melanoma Res* 2013;23(2):96–101. [PubMed: 23411479]
- Monteiro AC, Muenzner JK, Andrade F, Rius FE, Ostalecki C, Geppert CI, et al. Gene expression and promoter methylation of angiogenic and lymphangiogenic factors as prognostic markers in melanoma. *Mol Oncol* 2019;13(6):1433–49. [PubMed: 31069961]
- Nguyen GT, Gertz M, Steegborn C. Crystal structures of Sirt3 complexes with 4'-bromo-resveratrol reveal binding sites and inhibition mechanism. *Chem Biol* 2013;20(11):1375–85. [PubMed: 24211137]
- Niss Arfelt K, Barington L, Benned-Jensen T, Kubale V, Kovalchuk AL, Daugvilaite V, et al. EB12 overexpression in mice leads to B1 B-cell expansion and chronic lymphocytic leukemia-like B-cell malignancies. *Blood* 2017;129(7):866–78. [PubMed: 28003273]
- North BJ, Verdin E. Sirtuins: Sir2-related NAD-dependent protein deacetylases. *Genome biology* 2004;5(5):224. [PubMed: 15128440]
- Okamoto M, Liu W, Luo Y, Tanaka A, Cai X, Norris DA, et al. Constitutively active inflammasome in human melanoma cells mediating autoinflammation via caspase-1 processing and secretion of interleukin-1beta. *The Journal of biological chemistry* 2010;285(9):6477–88. [PubMed: 20038581]
- Olbryt M, Habryka A, Tyszkiewicz T, Rusin A, Cichon T, Jarzab M, et al. Melanoma-associated genes, MXI1, FN1, and NME1, are hypoxia responsive in murine and human melanoma cells. *Melanoma Res* 2011;21(5):417–25. [PubMed: 21912348]
- Ouyang L, Shen LY, Li T, Liu J. Inhibition effect of Oncostatin M on metastatic human lung cancer cells 95-D in vitro and on murine melanoma cells B16BL6 in vivo. *Biomed Res* 2006;27(4):197–202. [PubMed: 16971773]
- Overwijk WW, Restifo NP. B16 as a mouse model for human melanoma. *Curr Protoc Immunol* 2001;Chapter 20:Unit 20 1.
- Panza E, De Cicco P, Ercolano G, Armogida C, Scognamiglio G, Anniciello AM, et al. Differential expression of cyclooxygenase-2 in metastatic melanoma affects progression free survival. *Oncotarget* 2016;7(35):57077–85. [PubMed: 27494851]
- Patel SP, Kurzrock R. PD-L1 Expression as a Predictive Biomarker in Cancer Immunotherapy. *Mol Cancer Ther* 2015;14(4):847–56. [PubMed: 25695955]
- Petersen CC, Diernaes JE, Skovbo A, Hvid M, Deleuran B, Hokland M. Interleukin-21 restrains tumor growth and induces a substantial increase in the number of circulating tumor-specific T cells in a murine model of malignant melanoma. *Cytokine* 2010;49(1):80–8. [PubMed: 19962321]
- Pomyje J, Zivny JH, Stopka T, Simak J, Vankova H, Necas E. Angiopoietin-1, angiopoietin-2 and Tie-2 in tumour and non-tumour tissues during growth of experimental melanoma. *Melanoma Res* 2001;11(6):639–43. [PubMed: 11725211]

- Purwar R, Schlapbach C, Xiao S, Kang HS, Elyaman W, Jiang X, et al. Robust tumor immunity to melanoma mediated by interleukin-9-producing T cells. *Nat Med* 2012;18(8):1248–53. [PubMed: 22772464]
- Qin Y, Verdegaal EM, Siderius M, Bebelman JP, Smit MJ, Leurs R, et al. Quantitative expression profiling of G-protein-coupled receptors (GPCRs) in metastatic melanoma: the constitutively active orphan GPCR GPR18 as novel drug target. *Pigment Cell Melanoma Res* 2011;24(1):207–18. [PubMed: 20880198]
- Ruma IM, Putranto EW, Kondo E, Murata H, Watanabe M, Huang P, et al. MCAM, as a novel receptor for S100A8/A9, mediates progression of malignant melanoma through prominent activation of NF-kappaB and ROS formation upon ligand binding. *Clin Exp Metastasis* 2016;33(6):609–27. [PubMed: 27151304]
- Sade-Feldman M, Kanterman J, Klieger Y, Ish-Shalom E, Olga M, Saragovi A, et al. Clinical Significance of Circulating CD33+CD11b+HLA-DR- Myeloid Cells in Patients with Stage IV Melanoma Treated with Ipilimumab. *Clin Cancer Res* 2016;22(23):5661–72. [PubMed: 27178742]
- Sajadimajd S, Khazaei M. Oxidative Stress and Cancer: The Role of Nrf2. *Curr Cancer Drug Targets* 2018;18(6):538–57. [PubMed: 28969555]
- Schats KA, Van Vre EA, De Schepper S, Boeckx C, Schrijvers DM, Waelput W, et al. Validated programmed cell death ligand 1 immunohistochemistry assays (E1L3N and SP142) reveal similar immune cell staining patterns in melanoma when using the same sensitive detection system. *Histopathology* 2017;70(2):253–63. [PubMed: 27496355]
- Sebastian C, Satterstrom FK, Haigis MC, Mostoslavsky R. From sirtuin biology to human diseases: an update. *The Journal of biological chemistry* 2012;287(51):42444–52. [PubMed: 23086954]
- Seidl H, Richtig E, Tilz H, Stefan M, Schmidbauer U, Asslaber M, et al. Profiles of chemokine receptors in melanocytic lesions: de novo expression of CXCR6 in melanoma. *Human pathology* 2007;38(5):768–80. [PubMed: 17306330]
- Shannon P, Markiel A, Ozier O, Baliga NS, Wang JT, Ramage D, et al. Cytoscape: a software environment for integrated models of biomolecular interaction networks. *Genome Res* 2003;13(11):2498–504. [PubMed: 14597658]
- Singh CK, Chhabra G, Ndiaye MA, Garcia-Peterson LM, Mack NJ, Ahmad N. The Role of Sirtuins in Antioxidant and Redox Signaling. *Antioxid Redox Signal* 2018;28(8):643–61. [PubMed: 28891317]
- Singh CK, Chhabra G, Ndiaye MA, Siddiqui IA, Panackal JE, Mintie CA, et al. Quercetin-Resveratrol Combination for Prostate Cancer Management in TRAMP Mice. *Cancers (Basel)* 2020a;12(8):2141.
- Singh CK, George J, Chhabra G, Nihal M, Chang H, Ahmad N. Genetic Manipulation of Sirtuin 3 Causes Alterations of Key Metabolic Regulators in Melanoma. *Front Oncol* 2021;11:676077. [PubMed: 33937086]
- Singh CK, George J, Nihal M, Sabat G, Kumar R, Ahmad N. Novel downstream molecular targets of SIRT1 in melanoma: a quantitative proteomics approach. *Oncotarget* 2014;5(7):1987–99. [PubMed: 24743044]
- Singh CK, Panackal JE, Siddiqui S, Ahmad N, Nihal M. Combined Inhibition of Specific Sirtuins as a Potential Strategy to Inhibit Melanoma Growth. *Front Oncol* 2020b;10:591972. [PubMed: 33178616]
- Slominski AT, Kim TK, Takeda Y, Janjetovic Z, Brozyna AA, Skobowiat C, et al. RORalpha and ROR gamma are expressed in human skin and serve as receptors for endogenously produced noncalcemic 20-hydroxy- and 20,23-dihydroxyvitamin D. *FASEB J* 2014;28(7):2775–89. [PubMed: 24668754]
- Stanojevic I, Miller K, Kandolf-Sekulovic L, Mijuskovic Z, Zolotarevski L, Jovic M, et al. A subpopulation that may correspond to granulocytic myeloid-derived suppressor cells reflects the clinical stage and progression of cutaneous melanoma. *Int Immunol* 2016;28(2):87–97. [PubMed: 26391013]
- Su DM, Zhang Q, Wang X, He P, Zhu YJ, Zhao J, et al. Two types of human malignant melanoma cell lines revealed by expression patterns of mitochondrial and survival-apoptosis genes: implications for malignant melanoma therapy. *Mol Cancer Ther* 2009;8(5):1292–304. [PubMed: 19383853]

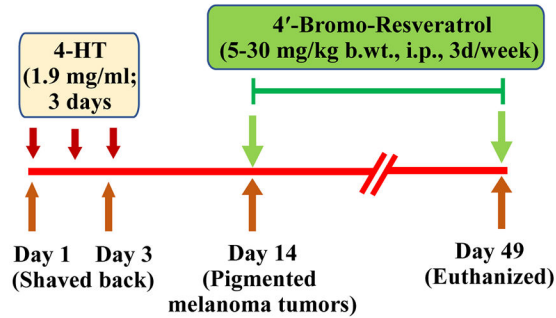


- Su S, Ndiaye M, Singh CK, Ahmad N. Mitochondrial Sirtuins in Skin and Skin Cancers. *Photochem Photobiol* 2020;96:973–980. [PubMed: 32124989]
- Sun S, Liu C. 7alpha, 25-dihydroxycholesterol-mediated activation of EB12 in immune regulation and diseases. *Front Pharmacol* 2015;6:60. [PubMed: 25852561]
- Szklarczyk D, Gable AL, Lyon D, Junge A, Wyder S, Huerta-Cepas J, et al. STRING v11: protein-protein association networks with increased coverage, supporting functional discovery in genome-wide experimental datasets. *Nucleic Acids Res* 2019;47(D1):D607–D13. [PubMed: 30476243]
- Terhorst D, Fossum E, Baranska A, Tamoutounour S, Malosse C, Garbani M, et al. Laser-assisted intradermal delivery of adjuvant-free vaccines targeting XCR1+ dendritic cells induces potent antitumoral responses. *J Immunol* 2015;194(12):5895–902. [PubMed: 25941327]
- Tu Y, Chen C, Fan G. Association between the expression of secreted phosphoprotein - related genes and prognosis of human cancer. *BMC cancer* 2019;19(1):1230. [PubMed: 31849319]
- Umansky V, Blattner C, Gebhardt C, Utikal J. CCR5 in recruitment and activation of myeloid-derived suppressor cells in melanoma. *Cancer Immunol Immunother* 2017;66(8):1015–23. [PubMed: 28382399]
- Vachharajani VT, Liu T, Wang X, Hoth JJ, Yoza BK, McCall CE. Sirtuins Link Inflammation and Metabolism. *J Immunol Res* 2016;2016:8167273. [PubMed: 26904696]
- Vilgelm AE, Pawlikowski JS, Liu Y, Hawkins OE, Davis TA, Smith J, et al. Mdm2 and aurora kinase a inhibitors synergize to block melanoma growth by driving apoptosis and immune clearance of tumor cells. *Cancer Res* 2015;75(1):181–93. [PubMed: 25398437]
- Vilgelm AE, Richmond A. Chemokines Modulate Immune Surveillance in Tumorigenesis, Metastasis, and Response to Immunotherapy. *Front Immunol* 2019;10:333. [PubMed: 30873179]
- Vitiello M, Evangelista M, Di Lascio N, Kusmic C, Massa A, Orso F, et al. Antitumoral effects of attenuated *Listeria monocytogenes* in a genetically engineered mouse model of melanoma. *Oncogene* 2019;38(19):3756–62. [PubMed: 30664692]
- Wagner NB, Weide B, Gries M, Reith M, Tarnanidis K, Schuermans V, et al. Tumor microenvironment-derived S100A8/A9 is a novel prognostic biomarker for advanced melanoma patients and during immunotherapy with anti-PD-1 antibodies. *J Immunother Cancer* 2019;7(1):343. [PubMed: 31806053]
- Wang J, Ding N, Li Y, Cheng H, Wang D, Yang Q, et al. Insulin-like growth factor binding protein 5 (IGFBP5) functions as a tumor suppressor in human melanoma cells. *Oncotarget* 2015;6(24):20636–49. [PubMed: 26010068]
- Wang Y, Su L, Morin MD, Jones BT, Mifune Y, Shi H, et al. Adjuvant effect of the novel TLR1/TLR2 agonist Diprovocim synergizes with anti-PD-L1 to eliminate melanoma in mice. *Proc Natl Acad Sci U S A* 2018;115(37):E8698–E706. [PubMed: 30150374]
- Waster P, Orfanidis K, Eriksson I, Rosdahl I, Seifert O, Ollinger K. UV radiation promotes melanoma dissemination mediated by the sequential reaction axis of cathepsins-TGF-beta1-FAP-alpha. *British journal of cancer* 2017;117(4):535–44. [PubMed: 28697174]
- Wilking MJ, Singh C, Nihal M, Zhong W, Ahmad N. SIRT1 deacetylase is overexpressed in human melanoma and its small molecule inhibition imparts anti-proliferative response via p53 activation. *Arch Biochem Biophys* 2014a;563:94–100. [PubMed: 24751483]
- Wilking MJ, Singh CK, Nihal M, Ndiaye MA, Ahmad N. Sirtuin deacetylases: a new target for melanoma management. *Cell Cycle* 2014b;13(18):2821–6. [PubMed: 25486469]
- Wong PF, Wei W, Gupta S, Smithy JW, Zelterman D, Kluger HM, et al. Multiplex quantitative analysis of cancer-associated fibroblasts and immunotherapy outcome in metastatic melanoma. *J Immunother Cancer* 2019;7(1):194. [PubMed: 31337426]
- Wu X, Giobbie-Hurder A, Liao X, Connelly C, Connolly EM, Li J, et al. Angiopoietin-2 as a Biomarker and Target for Immune Checkpoint Therapy. *Cancer Immunol Res* 2017;5(1):17–28. [PubMed: 28003187]
- Xiong TF, Pan FQ, Li D. Expression and clinical significance of S100 family genes in patients with melanoma. *Melanoma Res* 2019;29(1):23–9. [PubMed: 30216200]
- Xiong TF, Pan FQ, Liang Q, Luo R, Li D, Mo H, et al. Prognostic value of the expression of chemokines and their receptors in regional lymph nodes of melanoma patients. *J Cell Mol Med* 2020;24(6):3407–18. [PubMed: 31983065]

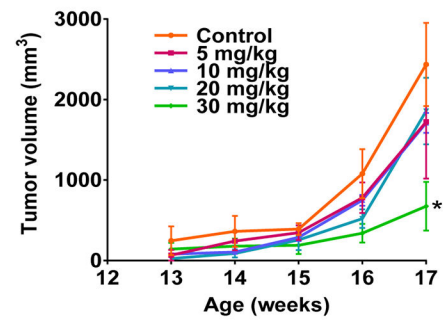
- Xu Y, Zhang F, Qin L, Miao J, Sheng W, Xie Y, et al. Enhanced in-vitro and in-vivo suppression of A375 melanoma by combined IL-24/OSM adenoviral-mediated gene therapy. *Melanoma Res* 2014;24(1):20–31. [PubMed: 24300090]
- Zhai Z, Liu W, Kaur M, Luo Y, Domenico J, Samson JM, et al. NLRP1 promotes tumor growth by enhancing inflammasome activation and suppressing apoptosis in metastatic melanoma. *Oncogene* 2017;36(27):3820–30. [PubMed: 28263976]
- Zhang Y, Ertl HC. Depletion of FAP+ cells reduces immunosuppressive cells and improves metabolism and functions CD8+T cells within tumors. *Oncotarget* 2016;7(17):23282–99. [PubMed: 26943036]
- Zhao B, Pritchard JR. Inherited Disease Genetics Improves the Identification of Cancer-Associated Genes. *PLoS Genet* 2016;12(6):e1006081. [PubMed: 27304678]

## a. Experimental design

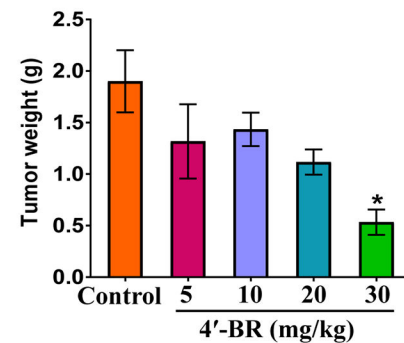
*BRAF<sup>V600E</sup>/PTEN<sup>Null</sup>* mice (n=30; Age 10 Wks;  
6 mice/group, 3 male and 3 females)

b. *BRAF<sup>V600E</sup>/PTEN<sup>Null</sup>* mice treated with 4'-BR

## c. Effect of 4'-BR on tumor volume



## d. Effect of 4'-BR on tumor weight



## e. Effect of 4'-BR on body weight

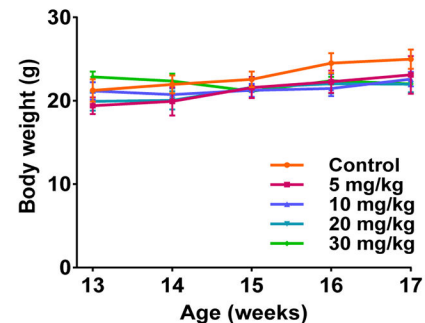


**Figure 1. 4'-BR significantly reduced melanoma tumor growth in *Braf<sup>V600E</sup>/Pten<sup>NULL</sup>* mice.** (a) Experimental design. (b) Representative images of *Braf<sup>V600E</sup>/Pten<sup>NULL</sup>* mice after treatments with 4'-BR (5-30 mg/kg b.wt.; intraperitoneally; 3d/week for 5 weeks) from each group at the end of the study (week 17). (c) Average tumor volume per group for weeks 13-17. (d) Average tumor weight per group at the end of study (week 17). (e) Average body weight per group for weeks 13-17. All data are presented as mean  $\pm$  standard error of the mean. \* $p < 0.05$ .

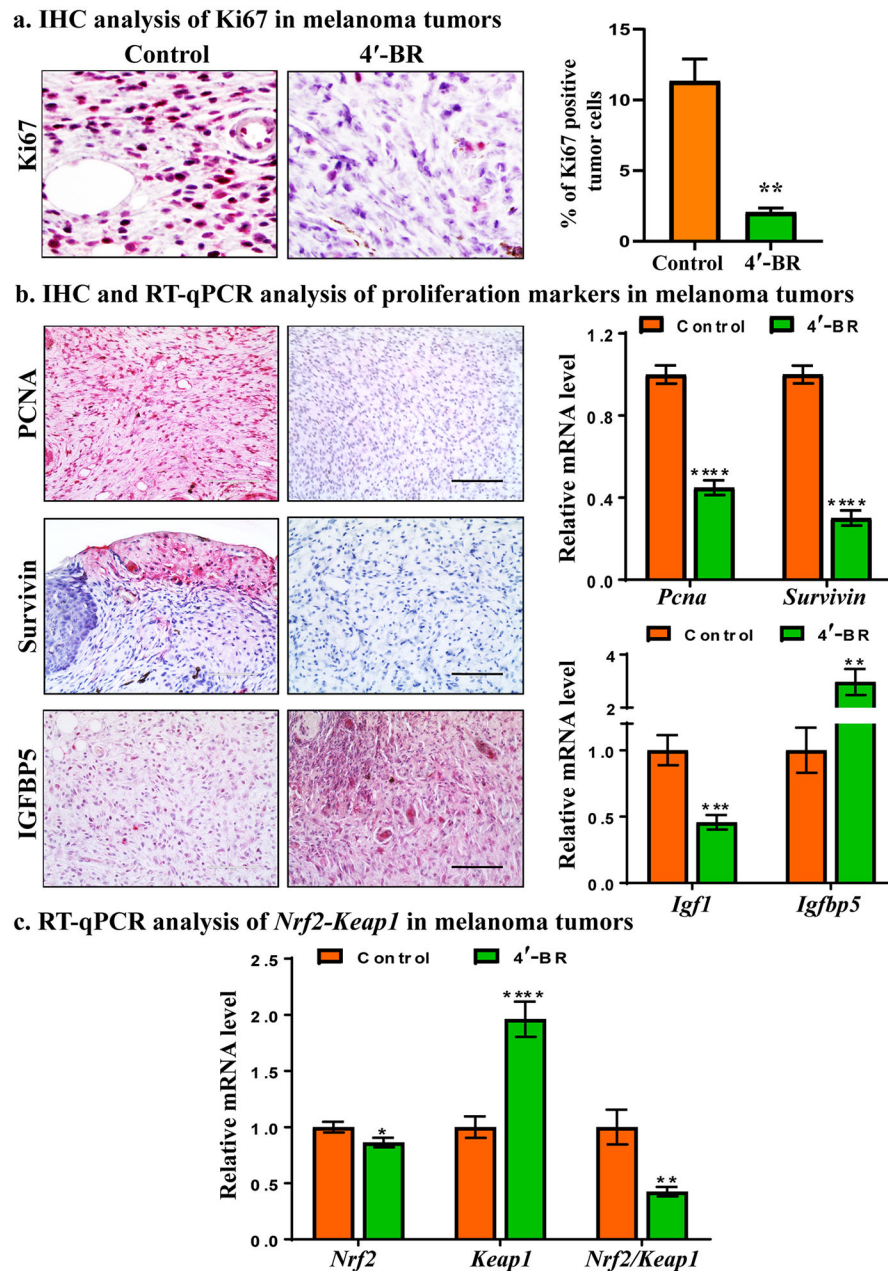
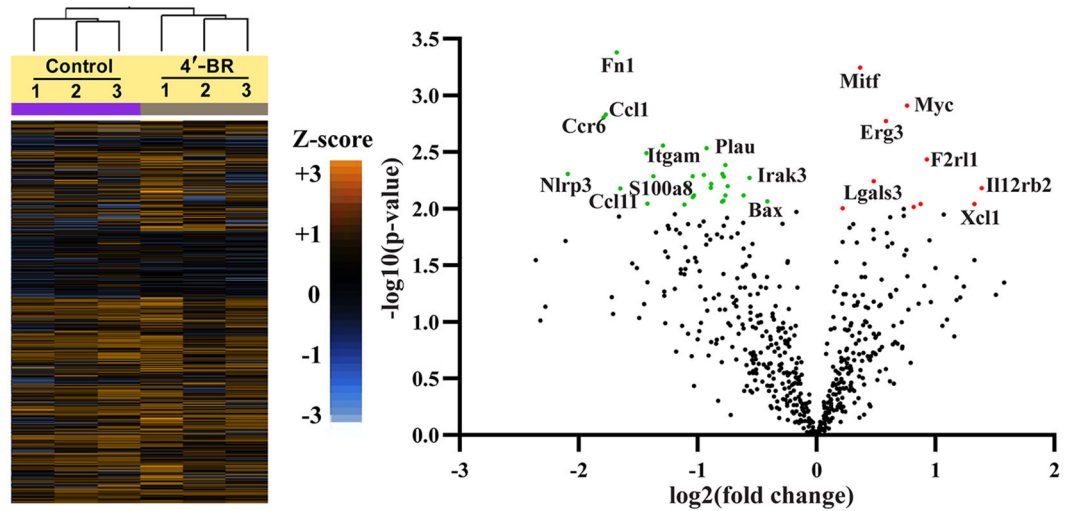


**Figure 2. 4'-BR significantly modulated cell proliferation, survival, growth factor signaling and oxidative stress markers in *Braf<sup>V600E</sup>/Pten<sup>NULL</sup>* mice.**

(a) Representative images of Ki67 protein expression by IHC (40X objective and 10X ocular) on an Olympus BX53 microscope. Each image is one quadrant (25%) of dimensions of 1360 x 1024 pixels. Ki67-positive tumor cells with bright red nuclear staining were counted manually. Stromal cells were excluded from counting. The fraction of Ki67-positive cells was determined as Ki67 positive tumor cells divided by total tumor cells. (b) Representative images of PCNA, Survivin, and IGFBP5 IHC (40x magnification, scale bars = 100  $\mu$ m) and relative mRNA levels of *Pcna*, *Survivin*, *Igf1*, and *Igfbp5* as determined by RT-qPCR. (c) mRNA expression analysis of activators of antioxidant response element, *Nrf2* and *Keap1* (by RT-qPCR) and their ratio. Data are presented as mean  $\pm$  standard error of

the mean, with statistical analysis performed using one-way analysis of variance with Tukey multiple comparisons. \* $P < 0.05$ , \*\* $P < 0.01$ , \*\*\* $P < 0.001$ , \*\*\*\* $P < 0.0001$ . Each bar represents a pool of six animals, as described in the Materials and Methods section. 4'-BR, 30 mg/kg body weight of 4'-bromo-resveratrol; IHC, immunohistochemistry.

a. Heat map and volcano plot of 770 cancer immune genes affected by 4'-BR treatment



b. Cancer immune pathways significantly affected by 4'-BR treatment

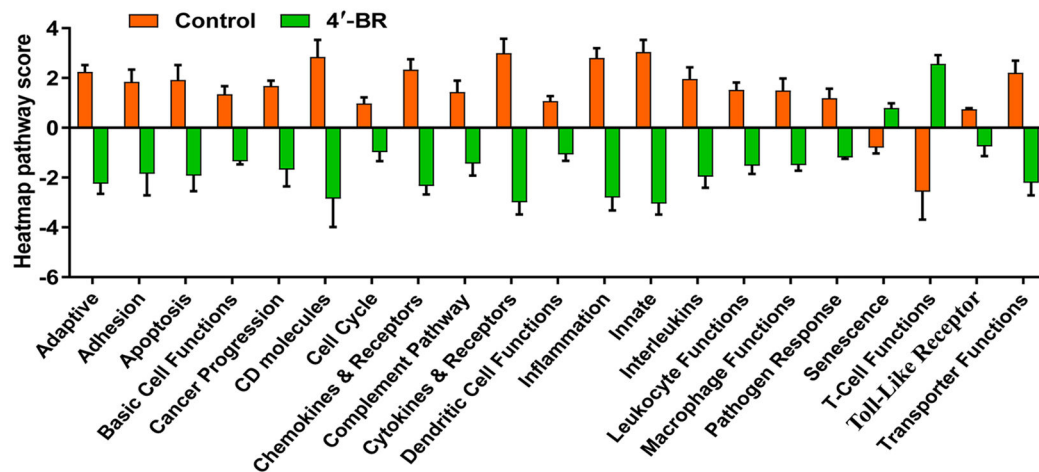


**Figure 3. 4'-BR significantly modulated genes associated with cancer immune signaling, as determined using NanoString PanCancer Immune Profiling Panel.**

RNA from primary tumor tissues of control and 4'-BR treated groups were subjected to NanoString analysis of 770 immune-related genes. (a) Left: Heatmap displaying each gene with color-coding for up- or down-regulation (orange and blue, respectively). Right: Volcano plots displaying each gene's  $-\log_{10}(P\text{-value})$  and log-two-fold change in 4'-BR treated group normalized with control group. Some of the most statistically significant genes are labeled in the plot. (b) Cancer immune pathways significantly ( $*P < 0.05$ ) modulated by 4'-BR treatment. Data are presented as mean  $\pm$  standard error of the mean ( $n=6$ ) of the pathway score.

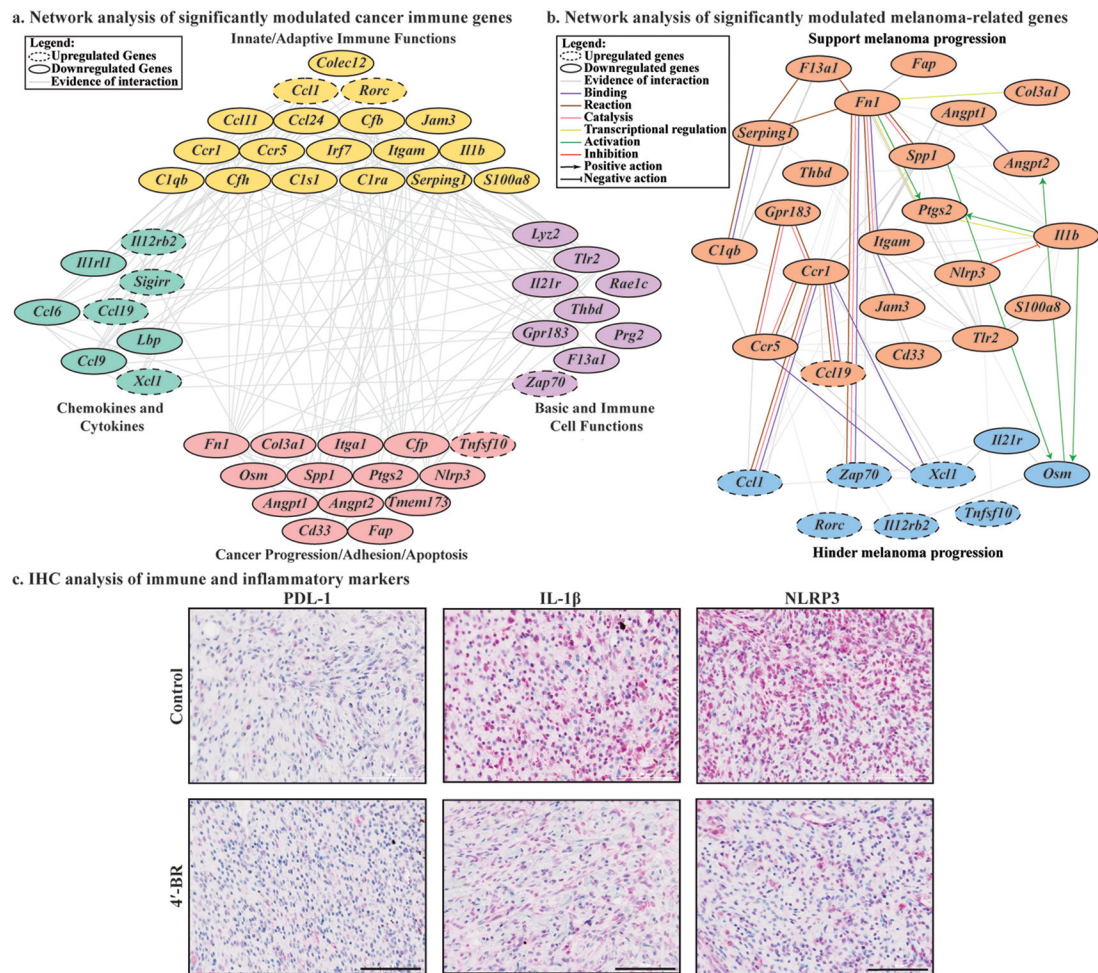


**Figure 4. 4'-BR significantly modulated immune genes/proteins that are interconnected and have supporting or suppressing roles in melanoma.**

Network analysis and IHC analysis were carried out as described in the Materials and Methods section. (a). Representative network of all differentially expressed genes. Genes were grouped according to their main functions provided by Nanostring as well as their GO term biological process. Gene roles include innate/adaptive immune functions (yellow/top group), basic and immune cell functions (purple/right group), chemokine/cytokines (green/left group), and cancer progression/adhesion/apoptosis (pink/bottom group). Grey lines indicate interactions. (b). Representative network of differentially expressed genes with previous evidence of being linked with melanoma. Genes were categorized according to previous evidence suggesting that they either support melanoma progression (orange) or hinder melanoma progression (blue). Downregulated genes have black solid outlines, while upregulated genes have black dashed outlines. Line color and termini indicate types of interactions: uncategorized evidence of interaction (grey), binding (purple), reaction (brown), catalysis (pink), transcriptional regulation (yellow), activation (green), inhibition (red), positive interaction (arrow), and negative interaction (bar-headed line). (c) IHC analysis of immune and inflammatory markers in 4'-BR treated *Braf*<sup>V600E</sup>/*Pten*<sup>NULL</sup> melanoma tumors. Representative images of PDL-1, IL-1 $\beta$ , and NLRP3 protein expression

by IHC (20X magnification, scale bars = 100  $\mu$ m) in a Lionheart FX automated microscope.  
4'-BR: 4'-bromoresveratrol (30 mg/kg body weight).

Author Manuscript

Author Manuscript

Author Manuscript

Author Manuscript



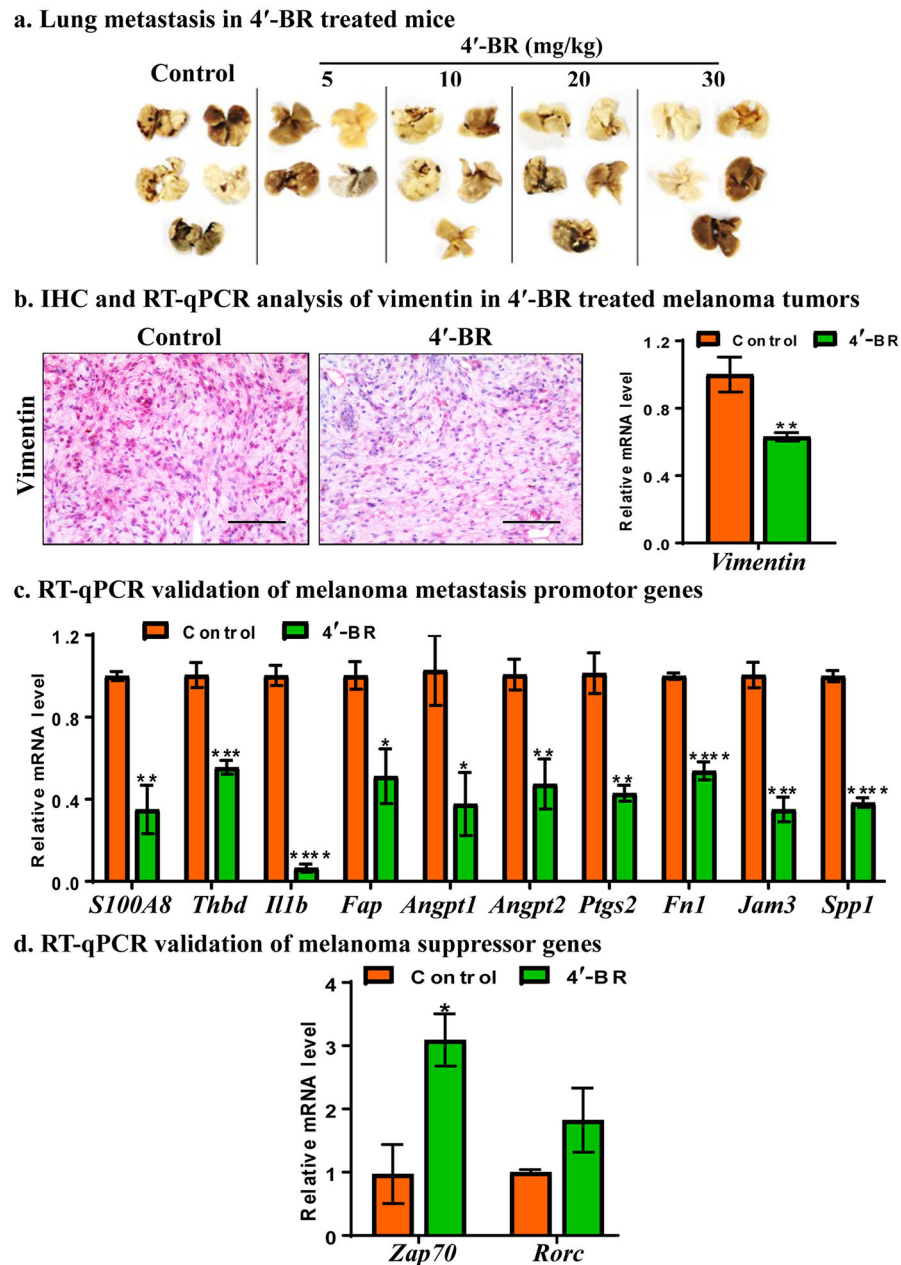


**Figure 5. 4'-BR significantly reduced melanoma metastasis in *Braf<sup>V600E</sup>/Pten<sup>NULL</sup>* mice.** (a) Lungs were harvested and stored in Fekete's solution at the end of study (week 17). Images of all collected lungs are shown. Data is available for 4-5 mice per group. (b) Expression of vimentin protein (by IHC, 40x magnification, scale bars = 100  $\mu$ m) and mRNA (by RT-qPCR). (c) RT-qPCR validation of melanoma promotor genes identified by NanoString analysis (d) RT-qPCR validation of melanoma suppressor genes identified by NanoString analysis. Data are presented as mean  $\pm$  standard error of the mean. \* $P < 0.05$ , \*\* $P < 0.01$ , \*\*\* $P < 0.001$ , \*\*\*\* $P < 0.0001$ . Each bar represents a pool of six animals, as described in the Materials and Methods section. 4'-BR, 30 mg/kg body weight of 4'-bromoresveratrol.

**Table 1.**

A detailed literature analysis of the 30 genes associated with melanoma and significantly affected by 4'-BR treatment in *Braf<sup>V600E</sup>/Pten<sup>NULL</sup>* mice.

Gene	Fold change	Gene functions in melanoma
FN1	-3.20	• Regulates EMT and blocks apoptosis; Promotes melanoma metastasis (Li et al., 2019, Olbryt et al., 2011).
CCR1	-3.40	• Present in melanocytes and melanoma cells; Expression increases with melanoma progression (Seidl et al., 2007).
ITGAM	-2.43	• Linked with more risk of melanoma (Lenci et al., 2012).
NLRP3	-4.25	• Enhances tumorigenesis (Zhai et al., 2017); Activates IL-1 $\beta$ secreted by advance stage melanoma cells (Okamoto et al., 2010); Inhibition diminishes migration and invasion (Lee et al., 2019).
S100A8	-2.58	• Enhances melanoma carcinogenesis (Ruma et al., 2016); Supports metastatic progression (Chen et al., 2019, Xiong et al., 2019); Higher expression in metastatic than primary melanoma (Wagner et al., 2019).
C1QB	-2.06	• Upregulated in blood samples of melanoma patients from all stages, especially in patient's leukocytes (Luo et al., 2011).
CD33	-2.13	• CD33 <sup>+</sup> myeloid-derived suppressor cells (MDSCs) are associated with increased risk of melanoma progression as well as less survival; A potential predictive and prognostic biomarker for advanced melanoma (Jordan et al., 2013, Sade-Feldman et al., 2016, Stanojevic et al., 2016)
F13A1	-2.04	• Highly expressed in advanced tumors and functions in blood coagulation cascade and resistance to treatments (Azimi et al., 2014).
IL1B	-8.19	• Expression increases with melanoma progression (Jiang et al., 2015); Upregulated in metastatic melanoma (da Silva et al., 2016).
FAP	-1.97	• Expressed at high levels in melanoma (Wong et al., 2019, Zhang and Ertl, 2016); Promotes metastasis by deteriorating the ECM, which helps cancer cells disseminate and invade other tissues (Waster et al., 2017).
JAM3	-2.36	• Associated with cell invasion and metastasis (Arcangeli et al., 2012); Expressed in metastatic melanoma cell lines (Ghislin et al., 2011).
COL3A1	-2.36	• Mutation in <i>Col3a1</i> gene is linked to melanoma progression and less survival (Zhao and Pritchard, 2016).
SERPING1	-2.27	• Forms part of a network formed by immune-related genes which in melanoma is dysregulated (Martins et al., 2011).
TLR2	-2.14	• Expressed in melanoma cells (Mauldin et al., 2015); Activates chemokines, cytokines, dendritic cells, and tumor-associated macrophages (Wang et al., 2018).
ANGPT2	-2.40	• Stimulates angiogenesis (Huang et al., 2017, Monteiro et al., 2019, Pomyje et al., 2001); A tumor promoter that can be used as a predictive and prognostic biomarker in melanoma; High expression is correlated with less survival; involved in resistance to treatments (Wu et al., 2017).
SPP1	-2.36	• <i>Spp1</i> gene is mutated in melanoma (Tu et al., 2019); Consistently upregulated in metastatic stages (Hill et al., 2015).
THBD	-2.02	• Loss is associated with tumorigenesis, invasion, and metastasis (de Oliveira Ada et al., 2014, de Wit et al., 2005, Furuta et al., 2005); Decreased levels are correlated with less survival (Hsu et al., 2012).
IL21R	-8.00	• A tumor suppressor gene progressed to clinical trials in metastatic melanoma for a plausible treatment (Davis et al., 2007); Can be used in combination with chemoimmunotherapy to improve the treatment response by increasing the tumor-specific T cells (Petersen et al., 2010).
OSM	-5.12	• In both early and advanced melanoma tumors and cell lines, this cytokine has tumor suppressive functions (Lazar-Molnar et al., 2000, Xu et al., 2014); Decreases cell adhesion and invasion both <i>in vitro</i> and <i>in vivo</i> in mouse metastatic cells (Ouyang et al., 2006).
ANGPT1	-2.19	• Play important role in angiogenesis and tumor development (Gardizi et al., 2012); However, ANGPT1 deficient mice exhibited increase in lung metastasis of B16F10 melanoma cells (Michael et al., 2017).
PTGS2	-1.97	• Commonly present in advanced melanomas, increases cell proliferation, migration, and invasiveness as well as promote tumor growth and metastasis (Ercolano et al., 2019); Elevated levels are significantly correlated with thicker melanomas as well as high proliferation and poor survival (Ercolano et al., 2019, Minisini et al., 2013, Panza et al., 2016).
GPR183	-2.15	• Upregulated in metastatic melanoma (Qin et al., 2011, Sun and Liu, 2015); High levels decrease immune responses, increases cell proliferation, and activate B-cell migration (Niss Arfelt et al., 2017).

Gene	Fold change	Gene functions in melanoma
CCR5	-2.68	<ul style="list-style-type: none"> <li>Associated with cancer progression and EMT with higher expression in melanoma cells (Liu et al., 2019, Umansky et al., 2017); Decreasing levels have inhibitory effects on primary tumors as well as metastasis (Liu et al., 2019); Stimulates MDSCs when inflammation occurs during melanoma progression (Blattner et al., 2018, Umansky et al., 2017).</li> </ul>
IL12RB2	2.62	<ul style="list-style-type: none"> <li>Acts as a tumor suppressor which activates immune responses and stops angiogenesis and even tumor growth (Airoldi et al., 2007); In invasive cells, expression decreases due to hypermethylation, which is associated with increased tumorigenesis (Koroknai et al., 2020).</li> </ul>
XCL1	2.52	<ul style="list-style-type: none"> <li>High expression is correlated with good prognosis (Xiong et al., 2020); It recruits dendritic cells (DCs) to tumors (de Andrade et al., 2019), slow down and protect against tumor growth and even cause tumor regression (Botelho et al., 2019, Terhorst et al., 2015).</li> </ul>
CCL1	2.52	<ul style="list-style-type: none"> <li>Both T cells and NK cells depend on CCL1 to activate immune reactions leading to antitumor effects (Klarquist et al., 2016, Vilgelm et al., 2015).</li> </ul>
ZAP70	2.00	<ul style="list-style-type: none"> <li>An immune response gene associated with longer patient survival (Bogunovic et al., 2009); Activated T cells with increased levels of ZAP70 leads to T cell toxicity against melanoma (Kong et al., 2009).</li> </ul>
RORC	2.27	<ul style="list-style-type: none"> <li>Expression decreases as melanoma progress, lowest expression in advanced stages and metastasis. High expression is correlated with good prognosis (Brozyna et al., 2016); A tumor suppressor which regulates local homeostasis (Fan et al., 2018, Slominski et al., 2014). High levels lead to inhibition of melanoma <i>in vivo</i> (Purwar et al., 2012).</li> </ul>
TNFSF10	3.00	<ul style="list-style-type: none"> <li>TNFSF10, a proapoptotic gene, decreased in melanoma cells suggesting it contributes to better survival and growth (Su et al., 2009); Induces an immune response and has a very high and selective capability to kill cancer cells (Eberle, 2019, Huang et al., 2020).</li> </ul>
CCL19	2.36	<ul style="list-style-type: none"> <li>Presence of CCL19, an immune and inflammation-related chemokine, is significantly associated with longer survival (Messina et al., 2012); Contributes to T cell and DCs survival as they migrate to the lymph nodes (Gonzalez et al., 2014, Vilgelm and Richmond, 2019).</li> </ul>